Cement and Concrete Research 40 (2010) 583–597

Contents lists available at ScienceDirect

Cement and Concrete Research

journal homepage: http://ees.elsevier.com/CEMCON/default.asp

Experimental investigation of the mechanisms by which $LiNO_3$ is effective against ASR

C. Tremblay [a], M.A. Bérubé [a,*], B. Fournier [a], M.D. Thomas [b], K.J. Folliard [c]

[a] Département de géologie et de génie géologique, Université Laval, Québec, QC, Canada G1K 7P4
[b] Department of Civil Engineering, University of New Brunswick, Fredericton, NB, Canada E3B 5A3
[c] Department of Civil Engineering, University of Texas, Austin, TX 78712, USA

ARTICLE INFO

Article history:
Received 5 November 2008
Accepted 24 September 2009

Keywords:
Alkali-silica reaction
Concrete expansion testing
Lithium nitrate
Lithium inhibition mechanisms
Reaction products

ABSTRACT

Various series of experiments were carried out on cements pastes, concretes made with a variety of reactive aggregates, composite specimens made of cement paste and reactive aggregate particles, and a variety of reactive natural aggregates and mineral phases immersed in various Li-bearing solutions. The main objective was to determine which mechanisms(s) better explain(s) the effectiveness of $LiNO_3$ against ASR and variations in this effectiveness as well with the type of reactive aggregate to counteract. The principal conclusions are the following: (1), the pH in the concrete pore solution does not significantly decrease in the presence of $LiNO_3$; (2), the concentration of silica in the pore solution is always low and not affected by the presence of $LiNO_3$, which does not support the mechanism relating to higher solubility of silica in the presence of lithium; (3), the only reaction product observed in the $LiNO_3$-bearing concretes looks like classical ASR gel and its abundance is proportional to concrete expansion, thus is likely expansive while likely containing lithium; this does not support the mechanisms relating to formation of a non or less expansive Si–Li crystalline product or amorphous gel; (4), early-formed reaction products coating the reactive silica grains or aggregate particles, which could act as a physical barrier against further chemical attack of silica, were not observed in the $LiNO_3$-bearing concretes, but only for a number of reactive materials after immersion in 1 N LiOH at 350 °C in the autoclave (also at 80 °C for obsidian); (5), higher chemical stability of silica due to another reason than pH reduction or early formation of a protective coating over the reactive phases, is the mechanism among those considered in this study that better explains the effectiveness of $LiNO_3$ against ASR.

1. Introduction

A few days after mixing, the micropores in hardened concrete are filled with a highly basic (i.e., pH ≥ 12.5) solution that consists mainly of dissolved alkali hydroxides (K^+, Na^+, and OH^- ions) with minor amounts of other elements (e.g., Si, Ca^{+2}, SO_4^{-2}) [1–3]. Poorly crystalline or metastable silica minerals (e.g. opal, tridymite, cristobalite), volcanic glass, micro- to cryptocrystalline quartz, and some varieties of macrogranular quartz within the aggregate particles are chemically unstable and react deleteriously in such high pH environment, sometimes inducing the premature distress of the affected concrete elements. This phenomenon is known as "alkali-silica reaction" (ASR).

The principal source of alkalies in conventional concrete is portland cement. The higher the dosage and the alkali content of the cement, the higher the total concrete alkali content, the higher the pH (or the OH ion concentration) in the pore solution, and the higher the risk of ASR in presence of potentially reactive aggregates. The chemical attack of reactive silica by the highly basic pore fluid results in the formation of an hygroscopic "alkali-silica gel" [3,4]. Portlandite releases OH^- ions in the concrete pore solution in order to satisfy equilibrium between the cations (mostly alkali ions) and the anions (mostly OH^- ions). Differences in free energy between this gel and the pore fluid would then induce water and various ionic species in the pore fluid to flow into this gel. The Ca^{+2} ions also play a critical role in the process [1,3]. Tensile stresses build up and microcracking occurs when the pressure generated at localized sites exceeds the tensile strength of the aggregate particles and of the cement paste. Concrete expansion develops with associated microcracking in the reactive aggregate particles and the cement paste.

Despite its name, the "alkali-silica gel" contains significant amounts of calcium [5]. Immersion tests in alkaline solution performed over the years in our laboratory on various calcium-free reactive silica materials (e.g. synthetic silica gel, quartzitic sandstone with quartz overgrowth

* Corresponding author.
E-mail address: ma.berube7@videotron.ca (M.A. Bérubé).

0008-8846/$ – see front matter © 2009 Elsevier Ltd. All rights reserved.
doi:10.1016/j.cemconres.2009.09.022

and so on) clearly demonstrated that large amounts of silica can dissolve and remain in solution until $Ca(OH)_2$ is incorporated into the system, which thus results in precipitation of a calcium-alkali-silica gel. Diamond [1] also observed that opal just dissolved in pure NaOH solution, then concluded that calcium (e.g. portlandite) is required for the formation of an expansive silica gel. It is also generally considered that other crystalline products of ASR are not deleteriously expansive [1]. It thus appears that the expansive/deleterious character of ASR products is largely influenced by their composition and degree of crystallinity.

McCoy and Caldwell [6] first proposed that the alkali-silica reactivity (ASR) could be controlled by using lithium admixtures. Since then, many studies showed that various lithium salts can reduce ASR expansion in concrete when used in sufficient amounts [7]. $LiNO_3$ proved to be one of the most effective salts. However, its effectiveness varies with the concrete alkali content and the type of reactive aggregate to counteract, irrespective of its inherent degree of expansivity (in control concretes) [8,9]. In fact, the mechanisms involved are still not well understood.

Various mechanisms can be proposed to explain the beneficial effect of $LiNO_3$ against ASR, which can be grouped in two main categories with respect to the two conditions required for deleterious expansion to occur in the presence of reactive silica, i.e. chemical attack of the silica by the highly basic concrete pore solution and formation of an expansive calcium-alkali-silica gel:

(1) The chemical stability of reactive silica is increased in the presence of $LiNO_3$, due to: (a) pH decrease in the concrete pore solution (mechanism A), (b) some other change(s) in the chemistry of this solution (mechanism B), and/or (c) early formation, at the surface of or somehow surrounding the reactive silica grains or aggregate particles, of a Si–Li reaction product, crystalline or amorphous, which acts as a physical barrier against further reaction (mechanism C);
(2) The chemical stability of reactive silica remains almost unchanged in the presence of $LiNO_3$, but concrete expansion is significantly reduced or suppressed, due to: (a) formation of a crystalline and non expansive Si–Li reaction product (mechanism D), (b) formation of a Si–Li amorphous gel which is, however, non expansive or much less expansive than the classical expansive ASR gel (mechanism E), or (c) higher solubility of silica, which thus allows most of the reacted silica to remain in solution without forming an expansive reaction product (mechanism F).

The mechanisms A to F are discussed hereafter.

1.1. Mechanism A — increased chemical stability of reactive silica due to pH decrease in the concrete pore solution

In the ASR, the aggressive ionic species against the reactive silica are the hydroxyl ions. As mentioned before, the portlandite ($Ca(OH)_2$) releases OH^- ions in the concrete pore solution in order to satisfy equilibrium between the cations (mostly alkali ions) and the anions (mostly OH^- ions), while the calcium ions play a critical role in the formation of an expansive gel. It could be suggested that the pH of the concrete pore solution is reduced in the presence of Li^+ cations. However, a number of studies already proved that the pH is not significantly modified in the presence of $LiNO_3$ [10–12]. For instance, in the study by Bérubé et al. [12] on cement pastes, the pH decreased by about 0.1 only in the presence of $LiNO_3$ with respect to control pastes. This was observed despite a higher overall [Na + K + Li] concentration in the pore solution, which was related to the addition of nitrate ions (not analyzed), which likely compete with the OH^- ions. The findings of Bérubé et al. [12] were similar to the results reported by Diamond [11].

1.2. Mechanism B — increased chemical stability of reactive silica due to some change (other than pH) in the chemistry of the concrete pore solution

Lawrence and Vivian [13] found that the dissolution of silica is influenced by the type of hydroxide involved, being lower in the presence of LiOH than with NaOH, the highest rate being observed with KOH. Wijnen et al. [14] also observed with the same trend that the dissolution of amorphous silica gel was greatly affected by the type of alkali hydroxide used and suggested that the dissolution rate decreases as the hydrated ionic radius increases, e.g. from K^+ (smallest hydrated ionic radius) to Na^+ to Li^+ (largest hydrated ionic radius). For their part, Collins et al. [15] observed a reduction in silica dissolution in the presence of $LiNO_3$ and LiCl, but an increase in the presence of LiOH (mixed with a solution of 0.7 M NaOH). It is likely that this increase was due to pH increase due to the addition of LiOH, as observed by Diamond [11]. In the study by Feng et al. [16], the amounts of silica dissolved and sodium consumed decreased with respect to the NaOH control solution when ground samples of various reactive aggregates were immersed in a $NaOH + LiNO_3$ solution. However, the authors [16] were not able to correlate the effectiveness of lithium, variable from one reactive aggregate to another, irrespective of their inherent degree of reactivity (i.e. expansion in control concretes), with the reduction of dissolved silica. All of the above results suggest that lithium can decrease the dissolution of silica, then limiting the rate of formation of the expansive ASR gel.

1.3. Mechanism C — increased chemical stability of reactive silica due to early formation, in contact with the reactive silica grains or aggregate particles, of a Si–Li reaction product which acts as a physical barrier against further reaction

This protective product could be either crystalline or amorphous (i.e. a gel). In the study by Mitchell et al. [17], opal particles were covered with a reaction product (possibly a Li-silicate) after immersion in a 1 N LiOH solution oversaturated with respect to Ca $(OH)_2$ (solid lime in excess). These authors suggested that ASR is inhibited and perhaps stopped in LiOH due to the formation of a protective layer of a non expansive lithium-bearing silicate on the surface of the reactive aggregate particles. Yin and Wen [18] also observed a layer of a product different from the classical ASR gel on the surface of opal particles immersed in LiOH, which could hypothetically acts as a protective barrier. Lawrence and Vivian [13] concluded that a lithium silicate likely forms in the presence of LiOH and opal, and that this product is less soluble and more stable than the classical ASR gel (which theory partly relates to mechanism D below). Due to its stability, these authors thus suggested that this product may form an insoluble coating that protects the reactive silica from further attack by other alkali hydroxides.

1.4. Mechanisms D and E — chemical stability of reactive silica almost unchanged or remaining significant but concrete expansion significantly reduced or suppressed due to formation of a non or less expansive Si–Li reaction product, crystalline (mechanism D) or amorphous (mechanism E)

This product could be either crystalline or amorphous (i.e. a non or less expansive gel). The most common mechanism proposed to explain the effectiveness of lithium against ASR is that the swelling capacity of the ASR gel formed is modified in the presence of lithium ions, which gel would be non or less expansive.

Sakaguchi et al. [19] measured the concentrations of alkalis (K, Na, and Li) in the pore solution of mortar bars expressed under high pressure. For mortar bars containing lithium, they observed that Li ions were consumed in greater proportion than K and Na ions, and that the [Li] decreased with time while the [K] and [Na] remained constant. On the other hand, the [K] and [Na] decreased with time in

control mortar bars without lithium. The authors [19] thus suggested the formation of a non expansive lithium-bearing product in place of a more expansive product containing greater amounts of Na and K. In the study by Diamond and Ong [20], mortar bars incorporating LiOH and reactive silica (Beltane opal and cristobalite) did not expand but were showing gel when observed under ultraviolet light after being treated with uranyl acetate. This reaction product was then considered non expansive. This study [20] thus also suggests that the effectiveness of lithium against ASR is related to the formation of a non expansive (amorphous or crystalline) lithium silicate in place of the classical expansive silico-calco-alkaline gel formed in the absence of lithium. According to Mo et al. [21], because having a smaller (unhydrated) ionic radius and a higher surface charge density, the Li^+ ions are more readily incorporated in the ASR reaction product than the Na^+ and K^+ ions, and the lithium-bearing ASR product formed is crystalline and non expansive. Kurtis and Monteiro [22] proposed that the beneficial effect of lithium against ASR expansion is attributed to reduction in the surface charge density of the alkali-silicate gel formed in the presence of lithium. In the presence of $LiNO_3$, Collins et al. [15] observed the formation of a silica-rich product which could be non expansive. In a solution of 0.7 N NaOH containing LiOH at different [Li]/[Na], Yin and Wen [18] also concluded that the dissolution of silica from opal grains was reduced with respect to a lithium-free solution and, based on SEM observation, that a compact protective layer made of a lithium-silica gel was formed on the surface of the opal grains.

The well-established electrical double-layer theory (EDL) controls the adsorption of ions near/on the surface of any particle. The colloidal particles of ASR gel are assumed to be negatively charged, therefore tend to be surrounded by a positively charged electrical double layer, the thickness of which depends on the surface charge, the ionic composition of the solution and the cations adsorbed. Prezzi et al. [23] used this theory to explain the expansion due to the ASR gel, then to explain the effect of various chemical additives used to counteract ASR [24]. According to these authors, two factors would play an important role in the swelling of a gel: (1), the valence and (2), the hydrated radius of the cations present in the double layer: the higher the valence of a given cation, the lesser the gel swells, and the larger the hydrated radius of this cation, the more the gel swells. Based on these two parameters, the authors [24] considered that the expansion of the gel should increase according to the following sequence of adsorbed cations: $Al^{3+} < Ca^{2+} < Mg^{2+} < K^+ < Na^+ < Li^+$. Accordingly, Li ions should then result in a gel more expansive than gels containing Na or K, which clearly does not agree with the well-known beneficial effect of lithium. The authors [24] thus suggested that the anomalous position of Li^+ in the above sequence, with respect to reality, could be related to the fact that Li ions are primarily sequestered by the cement hydrates, thus are not available for the ASR.

1.5. Mechanism F — chemical stability of reactive silica almost unchanged or remaining significant but concrete expansion significantly reduced or suppressed due to a higher solubility of silica, which thus mostly remains in solution without forming an expansive gel

Another possible mechanism is that Li ions significantly increase the solubility of the reactive silica in the concrete pore solution. Using an X-ray microscope to observe the ASR occurring in solutions containing lithium or not, Kurtis and Monteiro [22] observed that a lesser amount of gel was formed in the presence of lithium. The authors thus proposed that, when lithium is present in sufficient quantity, the repulsion between the colloidal particles of silica remains high, thus preventing their polymerization and the consequent formation of an expansive silica gel.

This experimental study was undertaken with the main objective of determining the most probable mechanism(s) explaining the beneficial effect of $LiNO_3$ in controlling expansion due to ASR. A better understanding of the actual mechanisms involved would greatly help in making decisions regarding the use of $LiNO_3$ in concrete incorporating aggregates susceptible to ASR, taking particularly into account the nature of the reactive aggregate to counteract.

2. Materials and methods

Various series of experiments have been carried out in the presence of $LiNO_3$ or not (controls) (1) on concrete specimens incorporating various aggregates of different compositions and degrees of reactivity (pore solution chemistry and microanalysis), (2) on pure cement pastes (pore solution chemistry), (3) on composite specimens made of cement paste and a variety of reactive aggregates (immersion tests in $NaOH+LiNO_3$ solutions), and (4) on particles of a variety of reactive aggregates, silica species, silicates, and volcanic glass (immersion tests in various alkaline and Li-bearing solutions). Lithium was used as: (1) a solution containing 30 wt.% $LiNO_3$ (Euclid Lifetime N), and (2) a solid pulverized product containing at least 98 wt.% of $LiOH–H_2O$ (Sigma-Aldrich).

2.1. Pore solution chemistry of cement paste and concrete specimens (test series no. 1)

As described elsewhere, cement paste cylinders, 40 mm in diameter by 65 mm in length [12] and concrete prisms, 75 by 75 by 300 mm in size [9], were made with or without $LiNO_3$ (aqueous solution added to the mixture water), using a constant water-to-cement ratio of 0.42, different [Li]/[Na + K] molar ratios (0 for controls, 0.56, 0.74, 1.11), different cements (0.51, 0.82, 1.25 wt.% Na_2O_e), and different alkali contents with respect to the cement (0.51 wt.% Na_2O_e using the low-alkali cement; 1.25 wt.% Na_2O_e using the low-alkali or the medium-alkali cement with NaOH or KOH addition, or the high-alkali cement). Twelve ASR-reactive natural aggregates (4 gravels, two siliceous limestones, two greywackes, one dolostone, one chloritic schist, one rhyolite, and one granitic rock) and one non reactive limestone aggregate, 5 to 20 mm in size, were used for making the concrete specimens according to CSA A23.2-14A [25] (similar to ASTM C 1293 [26]). The cement paste and concrete specimens were stored above water in sealed containers at various temperatures (23, 38, and 60 °C for cement pastes; 38 and 60 °C for concretes). At different times (3, 7, 28, and 91 days for cement pastes; up to one year for concretes stored at 38 °C, and up to 91 days for concretes tested at 60 °C), the pore solution was expressed under high pressure from the specimens (1000 MPa for cement pastes; 1400 MPa for concretes) using the procedure first described by Longuet et al. [2] and commonly used since then. The equipment used for expression in this study had a cylindrical chamber of 50 mm (1.97 in) in diameter by 90 mm (3.54 in) in length and the pore solutions were expressed from broken pieces of concrete or from entire paste cylinders. The solutions were diluted by 100X (20X for the analysis of Si) and chemically analyzed for Na, K, Li, and Si, by ICP-OES (model Perkin Elmer**).** Taking into account the dilution factor, the minimum detection limits are estimated to 0.4, 5, 10, and 0.5 ppm for Si, Na, K, and Li, respectively. The OH^- concentration was also determined by direct titration with standardized HCl down to the phenolphtalein end point, and the pH values were calculated accordingly.

2.2. Visual examination and microanalysis of concrete specimens (test series no. 2)

2.2.1. Visual examination and SEM observations

At different times/expansions, the concrete specimens tested in series no. 1 were visually examined under the stereomicroscope. Representative fragments of several concretes incorporating various reactive aggregates and containing $LiNO_3$ or not, were then examined in more details under the scanning electron microscope (SEM) (model

JEOL JSM 840) at a beam voltage of 15 kV and using an EDXA (energy dispersive X-Ray analyzer) for chemical analysis.

2.2.2. Visual examination under ultraviolet light after uranyl acetate treatment

After 2 years at 38 °C or 6 months at 60 °C, a large number (42) of the above concrete prisms, made with 12 reactive and one non-reactive aggregates, and incorporating $LiNO_3$ at a [Li]/[Na + K] of 0.74 or 0 (control concretes) [9], were broken perpendicular to their length in order to obtain a quite even broken surface which was then wetted with a solution of uranyl acetate, allowed to stand for a few minutes, then thoroughly washed with running water to remove the excess of solution, and observed under ultraviolet light, following procedure AASHTO T 299-93 [27]. In this test, alkalies present in amorphous gel from ASR are removed and replaced by uranyl ions thus allowing the gel to exhibit a green fluorescent color when exposed to ultraviolet light.

2.2.3. SIMS microanalysis

After 2 years at 38 °C, polished sections of two concretes were analyzed using the Micro-SIMS apparatus (Secondary Ion Mass Spectrometer equipped with a microbeam) of CANMET (Ottawa, Canada), for assessing the spatial distribution of lithium in concrete and particularly the presence of Li-bearing reaction products of any type (i.e. crystalline or amorphous) or composition (e.g. calcium content). These two concretes, both containing $LiNO_3$ at a [Li]/[Na + K] of 0.74 and not expanding after 2 years, were made with a non-reactive pure limestone and a highly-reactive rhyolite, respectively. In this technique, the emission signals correspond to ions that volatilized from the surface of the specimen tested under the destructive action of the ionic source beam. A Ga beam was used in this study at a current of 2 or 5 nA. The scanning mode (8 scans per image) was used to obtain distribution maps for Li, Si and Ca over the selected scanned area of the two polished concrete sections. Under the conditions used, the lateral resolution is much lower than 1 μm and the minimum limit of detection is significantly lower than 1 ppm.

2.3. Composite specimens of aggregate particles and cement paste immersed in NaOH + $LiNO_3$ solutions (test series no. 3)

2.3.1. Polished aggregate particles embedded in a $LiNO_3$-bearing cement paste, with the composite specimens immersed for 28 days in a NaOH + $LiNO_3$ solution at 80 °C

Particles from one glassy and highly-reactive volcanic rock (obsidian), one highly-reactive aggregate (rhyolite), and one moderately-reactive aggregate (granitic rock), 10/14 mm in size, were sawed and polished on one face (using a diamond paste of 15 μm at the last polishing step), then embedded in cement paste containing $LiNO_3$ at a [Li]/[Na + K] of 0.74. The composite specimens were then immersed at 80 °C in a 1 N NaOH + 0.74 N $LiNO_3$ solution ([Li]/[Na] = 0.74). After 28 days, the specimens were broken along the original polished aggregate interface, which was treated with a 10 wt.% HCl solution to remove the residual cement paste adhering to the surface. Both the polished aggregate surface and the cement paste surface in immediate contact were analyzed by X-ray diffraction (XRD) (model Philips PW1080) at a voltage of 40 kV, a current of 20 mA, using a Cu source (1.54059A), a continuous scan of 1°(2θ)/mn from 10° to 60° or 80°, and the software Jade 2.0 for data processing. Afterwards, all surfaces were examined under the SEM.

2.3.2. Polished sections taken from prisms made of aggregate particles and cement paste and immersed for 28 days in NaOH and NaOH + $LiNO_3$ solutions at 80 °C

Sections, 25 mm in thickness, were sawed perpendicularly to the length of prisms, 75 by 75 by 300 mm in size, made of cement paste and 10/14 mm particles of three reactive aggregates (rhyolite, Spratt limestone, and greywacke). These sections were polished on one (sawed) face, immersed in 1 N NaOH (control) and 1 N NaOH + 0.74 N $LiNO_3$ ([Li]/[Na] = 0.74) solutions at 80 °C, periodically examined under the stereomicroscope, and analyzed under the SEM after 28 days.

2.4. Aggregate particles immersed in Li-bearing solutions (test series nos. 4a to 4d)

2.4.1. Polished aggregate particles immersed in a 1 N LiOH solution for 1 h at 350 °C (in autoclave at 300 psi or 2070 kPa) or for 6 months at 80 °C (only obsidian, unpolished) (test series no. 4a)

To better visualize and to accelerate at the same time the chemical interactions taking place between reactive aggregates and lithium-based admixtures, particles of a highly-reactive volcanic glass (obsidian) and of 8 natural aggregates (see Table 1), were sawed, polished on one (sawed) face, and immersed for 1 h in a 1 N LiOH solution in the autoclave at 350 ºC (300 psi or 2070 kPa). In addition, one obsidian particle, unpolished but with a quite even surface, was immersed for 6 months in a 1 N LiOH solution at 80 °C. The polished surfaces were analyzed by XRD before and after immersion, while the obsidian particle immersed for 6 months in a 1 N LiOH at 80 °C was also observed under the SEM.

Table 1
Mineral phases detected by XRD on the polished surface of various materials before and after immersion for 1 h in a 1 N LiOH solution at 350 °C (300 psi or 2070 kPa in the autoclave).

Aggregates ([Li]/[Na + K] effective ratio[a])	Mineral phases observed on the polished surface (listed from the most to the least abundant)	
	Before autoclaving	After autoclaving[b]
Highly reactive aggregates or materials		
Obsidian	Amorphous glass (see Fig. 2)	**Li-silicate** (see Fig. 2)
Rhyolite (0.63)	Quartz, Na-feldspar, biotite (traces) (see Fig. 3)	Quartz, **Li-silicate, Na-feldspar,** biotite (traces) (see Fig. 3)
Spratt limestone (1.04)	Calcite, quartz	**Portlandite, c**alcite, quartz
Greywacke (>1.11)	Quartz, Na-feldspar, calcite, chlorite, muscovite (traces)	Quartz, Na-feldspar
Clayey limestone (>1.11)	Calcite, quartz, Na-feldspar, chlorite (traces)	**Portlandite,** calcite, quartz, chlorite, Na-feldspar (traces), **Li-silicate (traces)**
Moderately reactive aggregates		
Dolostone (0.61)	Dolomite, quartz, calcite	Dolomite, **Li-silicate,** calcite, quartz (traces)
Chloritic schist (>0.93)	Quartz, calcite, chlorite, Na-feldspar, muscovite (traces)	Quartz, **portlandite**, chlorite, muscovite (traces), calcite (traces)
Granitic rock (0.56)	Quartz, Na-feldspar, K-feldspar	Quartz, **Li-silicate,** Na-feldspar, K-feldspar
Non reactive aggregates		
Pure limestone	Calcite	Calcite, **portlandite, Li-carbonate**

[a] Based on the results from concrete prism tests [9].
[b] The mineral phases in bold are those of greater importance in the present study.

2.4.2. Polished aggregate particles immersed for 28 days in a 1 N NaOH + 0.74 N $LiNO_3$ solution at 80 °C (test series no. 4b)

Polished particles of the same 8 natural aggregates (see Table 1) were also tested for 28 days in a 1 N NaOH + 0.74 N $LiNO_3$ solution ([Li]/[Na] = 0.74) at 80 °C. The polished surfaces were analyzed by XRD before and after immersion.

2.4.3. Aggregate powders (150–300 μm) immersed for 28 days in various Li-bearing solutions at 60 °C (test series no. 4c)

The obsidian and 3 reactive aggregates (see Table 2) were finely ground. 20-g samples of 150–300 μm particles were immersed for 28 days in 40 ml of the following solutions at 60 °C: (1), 0.38 N NaOH + 0.30 N KOH (control); (2), 1 N LiOH; (3), 0.8 N (Na,K)OH + 0.28 N $LiNO_3$ ([Li]/[Na] = 0.35), and (4), 0.8 N (Na,K)OH + 0.59 N $LiNO_3$ ([Li]/[Na] = 0.74). The test containers were shaken manually for 1 min every day for the first 5 days, then every 3 days until 28 days. After 1, 3, 7, and 28 days, the solutions were sampled (1 mL) and chemically analysed for Na, K, and Li, by ICP-OES.

2.4.4. Dissolution of particles of volcanic glass (obsidian), silica varieties, silicate minerals, and natural aggregates immersed for 28 days in various Li-bearing solutions at 80 °C (test series no. 4d)

Particles of various reactive and non-reactive materials (see Table 3) were immersed for 28 days in the following solutions at 80 °C: (1) 1 N NaOH (control); (2), 1 N LiOH; (3), 1 N NaOH + 0.25 N $LiNO_3$ ([Li]/[Na] = 0.25), and (4), 1 N NaOH + 0.50 N $LiNO_3$ ([Li]/[Na] = 0.50). Opal and chalcedony particles were also immersed in 1 N NaOH with other $LiNO_3$ concentrations (i.e. 0.1, 0.2, and 0.3 N for chalcedony; 0.75 N and 1.0 N for opal), with a few particles also transferred in the 1 N NaOH control solution after 28 days in a 1 N NaOH + 0.5 N (chalcedony) or 1.0 N (opal) $LiNO_3$. Only one particle, weighing 1.0 g ± 0.1, was tested per container with 200 ml of test solution, supported on a plastic grid. After cleaning its surface with distilled water and drying for 3 h at 80 °C (which was always sufficient to reach mass equilibrium), its mass was periodically measured up to a maximum of 28 days, depending on the test solution used and the kinetics of dissolution, with a precision of 0.0001 g. XRD was also performed after the tests on reacted particles of opal and chalcedony.

3. Results and discussion

This study involved a large number of very different tests series, each of them involving very different materials (e.g. concrete, cement paste, pure aggregates), experimental conditions, and analytical techniques. In order to prevent any confusion, the results obtained for each series are presented and immediately discussed one series by one with respect to the various mechanisms proposed above to explain the effectiveness of $LiNO_3$ against ASR. Accordingly, for each test series (no. 1 to 4d), each mechanism (no. A to F) will be considered "likely", "possible", "non-conclusive", "unlikely", or "impossible", based on the results obtained. The conclusions drawn in this respect are summarized in Table 4, along with the rationale behind.

Table 2
Li consumption (in wt.%) after 28 days in the test solution when aggregate powders (150–300 μm) were immersed in various Li solutions at 60 °C.

Aggregates	Li consumed (wt.%)		
	1 N NaOH + 0.35 N $LiNO_3$	1 N NaOH + 0.74 N $LiNO_3$	1 N LiOH
Spratt limestone	36.4	74.9	56.3
Rhyolite	26.3	48.9	53.8
Chloritic schist	31.7	47.7	54.3
Obsidian	30.5	29.2	82.5

Table 3
Mass variation (in wt.%) of various aggregates and mineral phases (varieties of silica, volcanic glass, and feldspars) after 28 days in various Li solutions.

Materials ([Li]/[Na + K] effective ratio[a])	1 N NaOH (no Li)	1 N NaOH + 0.25 N $LiNO_3$	1 N NaOH + 0.5 N $LiNO_3$	1 N LiOH
Natural aggregates (all reactive except two)				
Pure limestone (non reactive)	−0.1	Not tested	Not tested	0.0
Spratt limestone (1.04)	−4.4	−0.9	−0.6	−0.1
Rhyolite (0.63)	−7.8	−1.3	−0.9	−2.3
Clayey limestone (>1.11)	−2.2	−0.9	−0.4	−0.1
Greywacke (>1.11)	−8.5	−0.9	−0.4	−1.0
Granitic rock (0.56)	−7.8	−1.3	−0.8	−1.8
Chloritic schist (>0.93)	−4.7	−0.1	+0.8	−0.1
Dolostone (0.61)	−1.1	−0.8	−0.4	−0.8
Quartz sandstone	−4.8	−0.7	+0.3	−1.2
Quartzite (non reactive)	−0.4	Not tested	Not tested	−0.4
Varieties of silica				
Quartz (non reactive)[b]	−0.1	Not tested	−0.1	0.0
Opal (amorphous silica)	−100.0	−100.0	−71.5	+9.4[d]
Chalcedony[c]	−100.0	−6.3	−0.1[e]	0.0[e]
Red chert[c]	−100.0	Not tested	+1.9	Not tested
Green chert[c]	−100.0	Not tested	−1.9	Not tested
Fused silica (synthetic)	−13.7	Not tested	+4.4[d]	−3.6
Volcanic glass and varieties of feldspars				
Obsidian (volcanic glass)	−7.8	Not tested	−7.0[d]	−10.2
Anorthite (non reactive)[b]	−0.7	Not tested	Not tested	−1.2
Microcline (non reactive)[b]	−0.4	Not tested	Not tested	−1.3
Orthoclase (non reactive)[b]	−1.8	Not tested	Not tested	−1.4

[a] Based on concrete prism tests [9].
[b] Fragment from a coarse crystal.
[c] Cryptocrystalline quartz.
[d] Li-silicate not observed on the particle tested.
[e] Li-silicate observed on the particle tested.

3.1. Pore solution chemistry of cement paste and concrete specimens (test series no. 1)

The main conclusions drawn from the chemical analyses of the pore solution of the cement paste and concrete specimens (details given in Bérubé et al. [12] and Tremblay et al. [9], respectively) are the following:

- The amount of Si in solution was always low with no significant differences between control and Li-bearing specimens. For instance, for the 8 sets of control concretes and concretes containing $LiNO_3$ at a [Li]/[Na + K] of 0.74, incorporating 4 different reactive aggregates (two siliceous limestones, one polygenic gravel, and one chloritic schist), stored at 38 °C, and tested at different expansion levels (from 28 up to 365 days of storage at 38 °C), the Si concentration averaged 0.0153 and 0.0135 mol/L for the control and Li-bearing concretes, respectively. On average, the [Si] is only slightly lower in the presence of $LiNO_3$.
- In the presence of $LiNO_3$ and after cement hydration has largely completed, i.e. after 91 days and even earlier, the [Li]/[Na + K] in the pore solution of all specimens investigated ranged between 0.30 and 0.45, which is about half of the original mixture ratio of 0.74. In fact, Li ions are incorporated in greater proportion than Na and K ions into the cement hydrates [12]. Consequently, the [Na + K] in the pore solution was significantly higher in the presence of $LiNO_3$ with respect to the control mixtures, while the pH was just slightly lower, by about 0.1. Nevertheless, the expansion due to ASR was largely reduced in the concretes incorporating reactive aggregates [9].
- In the presence of $LiNO_3$ at a [Li]/[Na + K] of 0.74, for all concretes tested and incorporating a variety of aggregates (non-reactive pure limestone, moderately-reactive Sudbury gravel for which $LiNO_3$ was very effective, moderately-reactive chloritic schist for which $LiNO_3$ was poorly effective (i.e. at the standard dosage of 0.74 and even more), and

Table 4
Summary of the degree of agreement between the results of test series nos. 1 to 4d and the mechanisms A to F proposed to explain the effectiveness of lithium against ASR.

Experiments (series #)	Agreement between the test results and the following mechanism proposed[a]					
	chemical attack of silica decreased due to mechanism			chemical attack of silica unchanged but expansion reduced due to mechanism		
	A (pH decrease)	B (Other chemical reason)	C (Si–Li protective coating)	D (Non-exp. Si–Li cryst. product)	E (Non/less-exp. Si–Li gel)	F (Increased solubility of silica)
1. Pore solution chemistry of cement pastes and concretes	Impossible (pH not affected by $LiNO_3$)	Not conclusive	Possible ([Li] decreases more rapidly with time in presence of reactive aggregates → possible formation of Si–Li products, which could be crystalline or amorphous, non to less expansive, and/or protective)			Impossible ([Si] always low and not affected by $LiNO_3$)
2. Examination/ microanalysis of concretes	Not conclusive (pH not measured)	Likely (just traces of Si-Li products when $LiNO_3$ is very effective)	Unlikely (protective coating not observed, Si–Li crystalline product not observed, amount of typical ASR gel proportional to concrete expansion, and absence or just traces of reaction products, limited to typical ASR gel, when $LiNO_3$ is very effective)			Not conclusive (Si not measured in solution)
3. Polished aggregates + cement paste in NaOH ± $LiNO_3$ at 80 °C	Not conclusive (pH not measured)	Likely (Si–Li reaction products not observed)	Unlikely (Si–Li reaction products not observed)			Not conclusive (Si not measured in solution)
4a. Polished aggregates in LiOH at 350 °C (autoclave) or 80 °C (obsidian only)	Not conclusive (pH not measured)	Not conclusive (Si–Li product absent on 3 of the 4 reactive aggregates but for which $LiNO_3$ is poorly effective in concrete)	Possible (crystalline Li_2SiO_3 covering obsidian and all 3 aggregates for which $LiNO_3$ is very effective in concrete, but tests in LiOH and with most of them performed at 350 °C)		Not conclusive (gel not observed but tests in LiOH, in absence of lime, and with most of them at 350 °C)	Not conclusive (Si not measured in solution)
4b. Polished aggregates in NaOH + $LiNO_3$ at 80 °C	Not conclusive (pH not measured)	Not conclusive (silica gel, undetectable by XRD, could be absent; SEM not done)	Not conclusive (protective gel, undetectable by XRD, could be present; SEM not done)	Unlikely (no crystalline product)	Not conclusive (non to less expansive gel, undetectable by XRD, could be present; SEM not done)	Not conclusive (Si not measured in solution)
4c. Ground aggregates in LiOH or (Na,K)OH + $LiNO_3$ at 60 °C	Non conclusive (pH not measured)	Unlikely (Li product always formed)	Possible (Li–product always formed, which could be protective)	Possible (cryst. or amorphous (no XRD nor SEM) finely-dispersed Li–product always formed, proportionally to Li consumption, but expansivity unknown)		Not conclusive (Si not measured in solution)
4d. Aggregates particles in NaOH + $LiNO_3$ or LiOH at 80°C (dissolution test)	Not conclusive (pH not measured)	Likely for most reactive materials (Si dissolution significantly reduced or suppressed)	Unlikely (significant coating only on opal, which is non-protective)	Unlikely (crystalline product only on undissolved chalcedony and very thin)	Possible for some materials (finely–disp. amorphous product ∞ to dissolution but expansivity unknown)	Not conclusive (Si not measured in solution)
Overall conclusion	Impossible	Likely	Unlikely	Unlikely	Unlikely	Impossible

[a] Mechanism: likely, posible, not conclusive, unlikely, or impossible, based on the test results.

highly-reactive Spratt limestone for which $LiNO_3$ was also poorly-effective), the [Li] in the pore solution decreased continuously with time, much more rapidly in the presence of reactive aggregates, and even after 91 days, i.e. after cement hydration has largely completed [9].

3.1.1. Discussion

The results of test series no. 1 clearly indicate that, since the pH in the pore solution is not significantly reduced in the presence of $LiNO_3$ and that the Si concentration in the pore solution is not modified in the presence of $LiNO_3$, mechanisms A and F are not possible. Considering that, all other test series did not involve any measurement of pH and Si concentrations in solution, these two mechanisms will not be considered in the following until the general discussion of Section 3.8. For its part, the significantly lower [Li] observed in the presence of reactive aggregates suggests the formation of some Si–Li reaction products, which could be crystalline or amorphous, expansive or not, and/or protective against ASR. Consequently, the mechanisms C (protective product), D (non expansive crystalline product) and E (non to less expansive gel) remain possible based on this set of data.

3.2. Visual examination and microanalysis of concrete specimens (test series no. 2)

3.2.1. Visual examination and SEM observations

Significant amounts of characteristic reaction products from ASR (siliceous gel and microcrystalline products) were observed visually and under the SEM in the control concretes showing high expansion, i.e. in the absence of $LiNO_3$. On the other hand, an amorphous gel containing Si, Ca, Na, and K, and possibly also Li (lithium cannot be detected in SEM as its characteristic X-ray wavelength is out of most EDS and WDS detectors' range), was the only reaction product observed in the $LiNO_3$-bearing concretes, but always in much lower amounts than in corresponding control concretes, without any noticeable difference in morphology and (detectable) chemical composition with respect to the classical ASR gel (observed in the control concretes). Moreover, no other type of reaction product was observed at the surface of the reactive aggregate particles (as a potentially protective coating) or elsewhere in the cement paste. These observations apply, whatever the reactive aggregate used and the effectiveness of $LiNO_3$ in its respect.

3.2.2. Visual examination under ultraviolet light after uranyl acetate treatment

The amounts of alkali-silica-gel observed under ultraviolet light on the broken sections of control and Li-bearing concretes after the application of uranyl acetate always seemed to be proportional to concrete expansion (due to ASR), whatever the reactive aggregate in concrete. This suggests that this gel is similarly expansive in both control and Li-bearing concretes, but present in much lower amounts in the latter. For instance, for all concretes made with $LiNO_3$ and showing no or limited expansion, no or only traces of reaction gel were observed under the ultraviolet illumination after uranyl acetate

treatment. These results disagree with Diamond and Ong [20] who observed, after uranyl acetate treatment, that significant amounts of reaction gel were present in non-expanding mortar bars containing lithium, however in the form of LiOH.

3.2.3. SIMS microanalysis

The micro-SIMS analyses showed that the atomic element Li was regularly distributed everywhere within the cement paste of the two concretes examined, containing reactive and non-reactive aggregates, respectively, without any particular/noticeable local concentrations in the cement paste, in the aggregates or along the aggregate/cement paste interfaces (Fig. 1).

3.2.4. Discussion

It is likely that most of the lithium detected with the micro-SIMS has precipitated from the pore solution when the test specimens were dried for analysis. In other words, it was not possible to detect the presence of Li-bearing reaction products in the concretes tested, (which would correspond to areas with a higher brightness on the Li images of Fig. 1, if present), even in the concrete made with the highly-reactive rhyolite and for which $LiNO_3$ was very effective in controlling expansion due to ASR [9].

The results of test series no. 2 from all visual and microscopic examinations on concrete specimens are in total agreement with each other. They do not support mechanisms D and E (which would call, in the presence of lithium admixtures, for the formation of significant amounts of non to less expansive crystalline or amorphous Li-bearing reaction products), and mechanism C as well (since the presence of a protective reaction product was not observed/detected at the surface of the reactive silica grains or aggregate particles, even when using the micro-SIMS technique). They rather support mechanism B, i.e. silica dissolution significantly reduced/suppressed but not due to mechanism A (since the pH is not affected by $LiNO_3$) or C (since a protective product was not observed). Indeed, in the presence of lithium and reactive aggregates, the lower the concrete expansion due to ASR, the lower the amount of (likely expansive) reaction gel observed in concrete, which suggests in turn that the reactive silica is more stable in the presence of lithium.

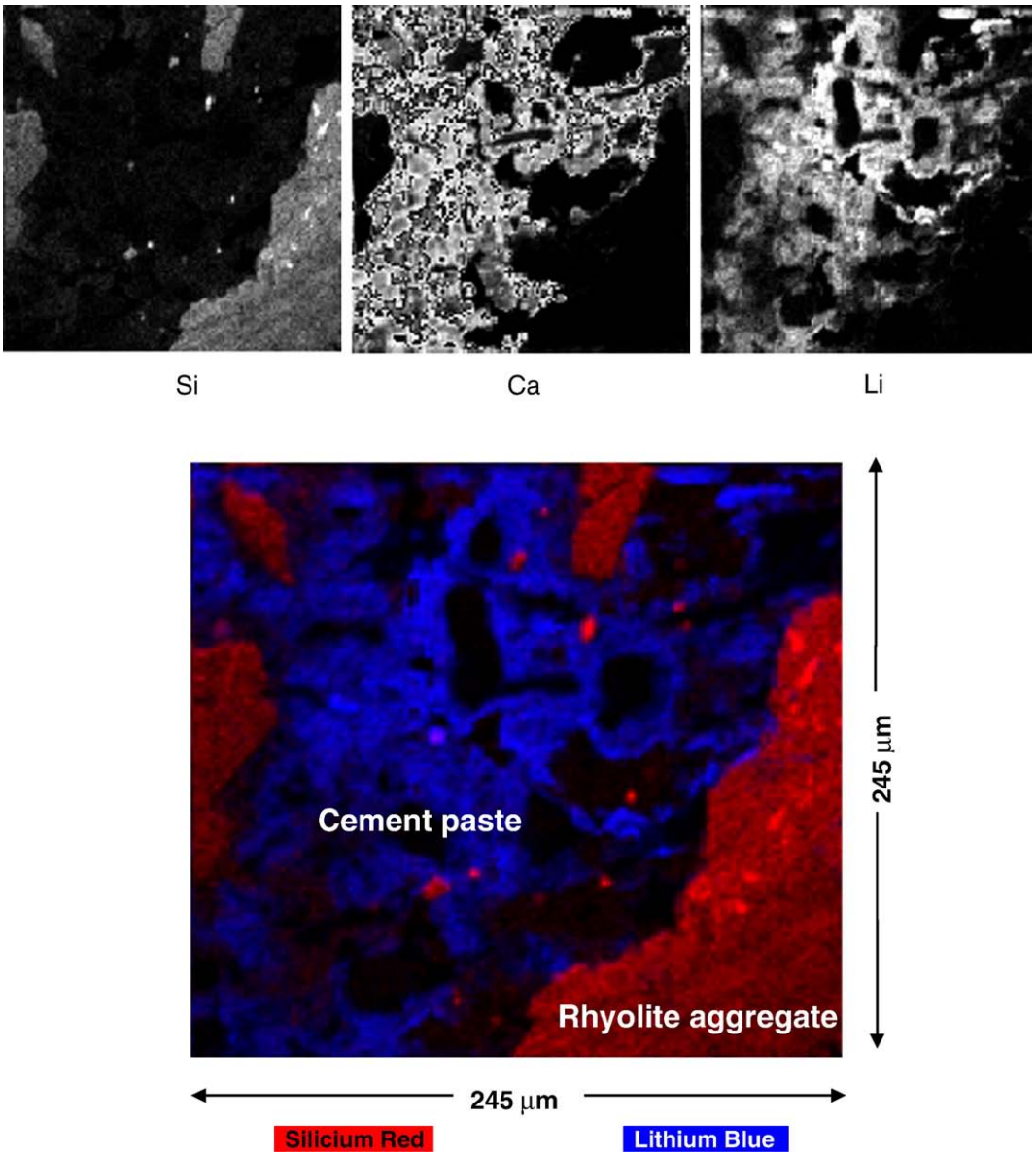

Fig. 1. Micro-SIMS elemental scans on a polished section of a concrete made with a highly reactive rhyolite and a [Li]/[Na + K] of 0.74, after 2 years at 38 °C and > 95% R.H. (0.01 vol.% expansion).

3.3. Composite specimens of aggregate particles and cement paste immersed in NaOH + $LiNO_3$ solutions (test series no. 3)

3.3.1. Polished aggregate particles embedded in a $LiNO_3$-bearing cement paste, with the composite specimens immersed for 28 days in a NaOH + $LiNO_3$ solution at 80 °C

Reaction products (crystalline and amorphous) were not detected by XRD neither observed under the SEM on the polished surface of the reactive aggregate particles tested nor on the surface of the cement paste in contact with the polished aggregate surfaces during immersion.

3.3.2. Polished sections taken from prisms made of aggregate particles and cement paste and immersed for 28 days in NaOH and NaOH + $LiNO_3$ solutions at 80 °C

Typical ASR gel was observed on the exposed polished surfaces of all reactive aggregate particles after immersion in the NaOH control solution. However, reaction products (crystalline or amorphous) were not observed after immersion in the $LiNO_3$-bearing solution.

3.3.3. Discussion

The results of test series no. 3 do not support mechanisms C, D, and E, since reaction products were not observed along the aggregate/cement paste interfaces (first sub-series of tests) neither on the polished sections of aggregate particles and cement paste in direct contact with the Li-bearing solution (second sub-series of tests). However, in this particular test series, the absence of any Li–Si reaction product (which does not support mechanisms C, D and E), rather supports mechanism B, i.e. increased stability of silica, particularly when considering that the specimens from the first sub-series were real hydraulic mixtures (i.e. incorporating cement and portlandite) for which it has been already proved that the pH is not significantly reduced (mechanism A impossible) and the solubility of silica is not affected by the presence of $LiNO_3$ (mechanism F impossible).

3.4. Aggregate particles immersed in a 1 N LiOH solution (test series no. 4a)

3.4.1. Polished aggregate particles immersed for 1 h in a 1 N LiOH solution at 350 °C (in the autoclave)

Table 1 gives the mineral phases detected by XRD, before and after autoclaving, on the polished surface of the 8 natural aggregates tested. After autoclaving, a crystalline Li-silicate, Li_2SiO_3, was detected by XRD on the polished surfaces of obsidian (Fig. 2) and the 3 reactive aggregates tested for which $LiNO_3$ proved to be effective in concrete, i.e. rhyolite (see Fig. 3), dolostone, and granitic rock, using a [Li]/[Na + K] < 0.74 [9] (Table 1). Li_2SiO_3 was also detected, however just in traces, on the surface of one (i.e. clayey limestone) of the 4 other reactive aggregates tested, for which a greater $LiNO_3$ content was needed in concrete to control ASR expansion, i.e. a [Li]/[Na + K] > 0.93 or more [9] (Table 1); it was not detected, however, for the three other aggregates (Spratt limestone, greywacke, chloritic schist) (Table 1). Secondary portlandite was also detected after autoclaving on the surface of all aggregates containing calcite in large amounts (i.e. Spratt limestone, clayey limestone, chloritic schist, and the non-reactive pure limestone), a Li-carbonate being even found on the pure limestone (Table 1). One could argue that a relatively thick layer of portlandite could explain that Li-silicate was not detected by XRD or just detected in traces in the case of 4 of the 7 reactive aggregates tested; however, one of these aggregates (greywacke) does not contain significant amounts of calcite while not showing portlandite after autoclaving.

3.4.2. Obsidian particle immersed for 6 months in a 1 N LiOH solution at 80 °C

After immersion, the obsidian surface was covered with a layer of crystalline Li_2SiO_3 (Fig. 4), identified by XRD. The presence of a continuous gap between the Li_2SiO_3 layer and the obsidian surface, which appears very smooth and microtexturally-unchanged with respect to the original material (Fig. 4), suggests that this "coating" product precipitated from the soak solution after some silica was dissolved rather to be a residual product left aside after the soak solution reacted with the obsidian. On the other hand, the absence of any significant sign of corrosion on the obsidian surface suggests that the dissolution of this material proceeded very regularly and at a very-fine scale all over the surface exposed to the soak solution. A finely-dispersed white product (not analyzed) was also observed at the bottom of the test containers, which may be crystalline or amorphous in nature, and expansive or not.

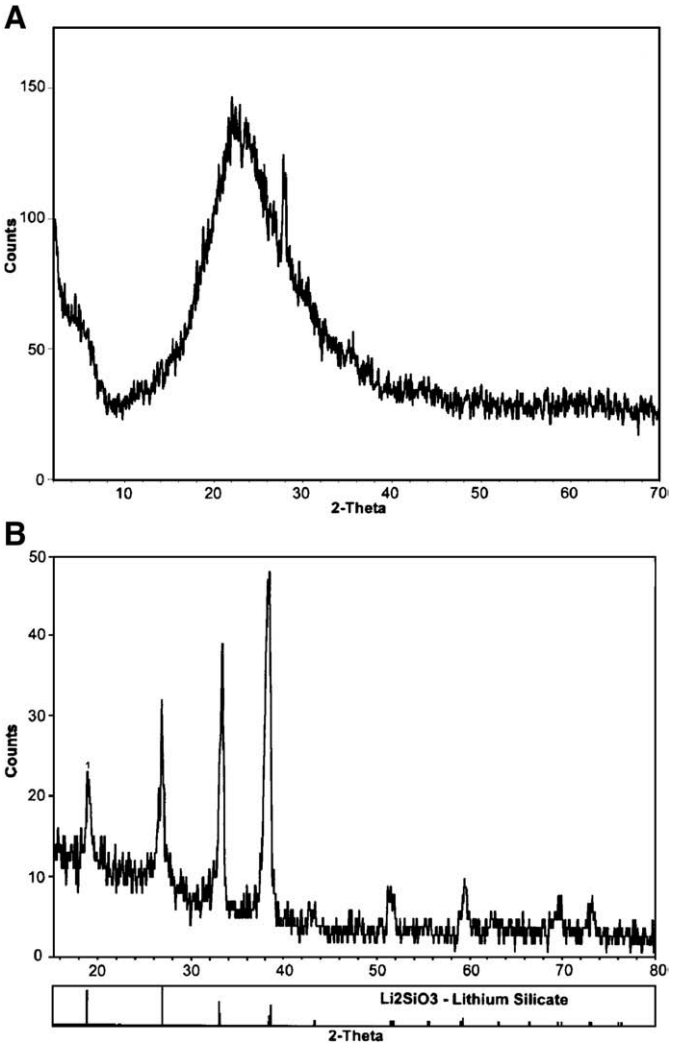

Fig. 2. XRD analysis of a polished section of obsidian before (A) and after (B) 1 h of autoclaving in a 1 N LiOH solution at 300 psi or 2070 kPa (350 °C). (A) The obsidian is mostly composed of amorphous glass. (B) The obsidian surface is covered by a layer of crystalline lithium silicate Li_2SiO_3 (ICDD card file 29-0829).

3.4.3. Discussion

The results from test series no. 4a suggest that a crystalline Li-silicate (Li_2SiO_3) can form in the presence of reactive aggregates for which $LiNO_3$ is effective in controlling concrete prism expansion using a [Li]/[Na + K] of 0.74 or less, however not in the presence of reactive aggregates for which $LiNO_3$ is needed in greater proportions for expansion control. They thus support, to some extent, mechanisms C and D (crystalline Si–Li reaction product observed on obsidian and 4 of the 7 reactive aggregates tested, which could be also protective). However, with respect to $LiNO_3$, these mechanisms are considered

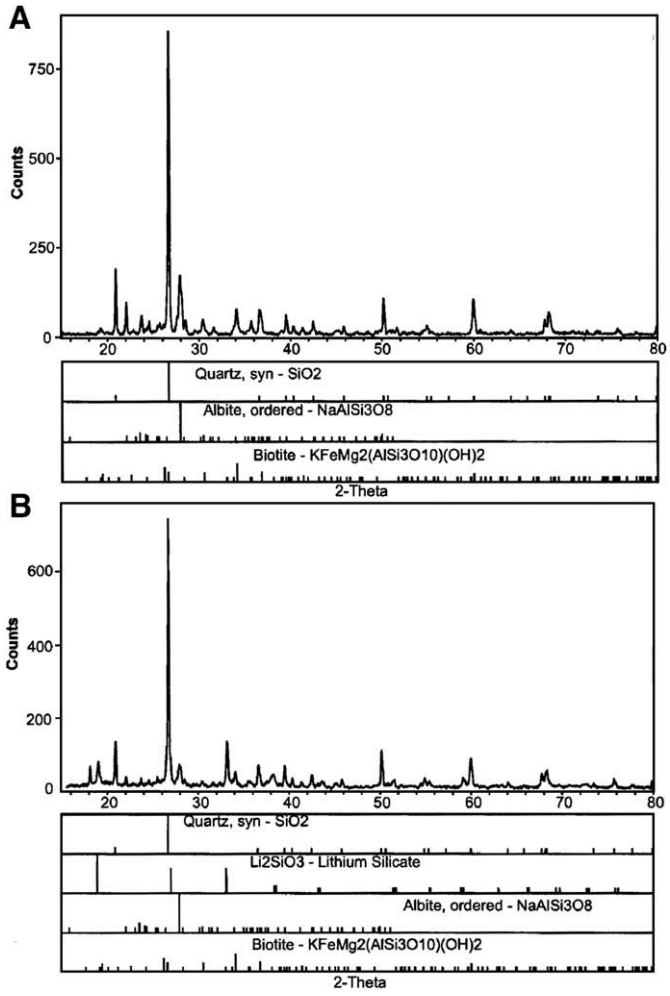

Fig. 3. XRD analysis of a polished section of a highly reactive rhyolite before (A) and after (B) 1 h of autoclaving in a 1 N LiOH solution at 300 psi or 2070 kPa (350 °C). After autoclaving (B), a crystalline lithium silicate Li_2SiO_3 (ICDD card file 29-0828) is detected on the rhyolite surface.

possible but uncertain considering that all tests involved special testing conditions (i.e. performed in a 1 N LiOH solution and at 350 °C for most of them).

3.5. Polished aggregate particles immersed for 28 days in a 1 N NaOH + 0.74 N $LiNO_3$ solution at 80 °C (test series no. 4b)

Polished particles of the 8 natural aggregates tested in the autoclave were also immersed for 28 days in a NaOH + 0.74 N $LiNO_3$ solution at 80 °C. For each aggregate, the XRD results were exactly the same before and after immersion, no crystalline Li-bearing product being detected on the polished surfaces.

3.5.1. Discussion

These results from test series no. 4b do not support at least mechanism D (since the presence of a crystalline product was not detected by XRD). Moreover, no other types of reaction product were observed in the test solutions, neither at the bottom of the test containers. At this stage of the study, it is thus possible that the crystalline Li-silicate observed in test series no. 4a just forms in LiOH (e.g. for obsidian in the long term at 80 °C) and under special conditions for some reactive aggregate particles (i.e. very high temperature and pressure in the autoclave). In the present experiment, there is a possibility that an amorphous Li-bearing gel, undetectable by XRD, formed at the surface of the polished particles rather than a crystalline product. Since the particles tested were not examined after the tests (e.g. using the SEM), one cannot thus conclude about mechanism B (amorphous gel could be absent), mechanism C (amorphous gel could be present which may act as a protective coating), and mechanism E (amorphous gel could be present, which could be non to less expansive).

3.6. Aggregate powders (150–300 μm) immersed for 28 days in various Li-bearing solutions at 60 °C (test series no. 4c)

When aggregate powders (150–300 μm) were immersed for 28 days in (Na,K)OH control solutions at 60 °C, the K and Na concentrations in the (Na,K)OH control solution were quite constant in the presence of all 4 materials tested, even the most reactive obsidian (Fig. 5A). For the materials immersed in the LiOH solution, the [Li] in solution decreased for each material, however more rapidly for obsidian (Fig. 5B). As illustrated in Fig. 5C and D for rhyolite, but also for each of the materials tested, the [Na] and [K] in the two (Na,K)OH + $LiNO_3$ solutions were quite stable over time, while the [Li] significantly decreased, more rapidly in the solution with higher concentration of $LiNO_3$ (Fig. 5C vs. D). The consumption of Li after 28 days is given in Table 2. In the presence of lithium, a finely-dispersed whitish product was always observed in the test containers.

3.6.1. Discussion

These results are in good agreement with those from pore solution chemistry of concretes (Section 3.1) where Li ions were consumed more rapidly than Na and K ions; the only difference is that in the concretes tested, Na and K ions were also progressively consumed with time (i.e. disappeared from the pore solution), due to alkali-leaching and to formation of more Li-Na–K-bearing cement hydrates, and expansive gel due to ASR as well. In the present case, cement was not present in the system and Li was still progressively consumed with time.

The results concerning the Li consumption (Table 2) clearly suggest that a secondary Li-bearing reaction product is formed. As mentioned above, a finely-dispersed whitish product was effectively always observed in the presence of lithium. The largest quantity was obtained for the obsidian immersed in the LiOH solution and also corresponds to the largest Li decrease in solution (~83 wt.% after 28 days; Table 2). Unfortunately, this product was not chemically analyzed neither analyzed with the SEM or by XRD; it could thus be crystalline or amorphous but it likely contains, in addition to Li, some Si, Na, and K. The important difference observed between series 4b (where no reaction product were detected) and series 4c (where a reaction product was always present in the presence of lithium solution) is likely attributed to extreme differences in specific area (i.e. single polished aggregate particles vs. aggregate powders).

It is not possible to conclude about a possible influence of the reactive aggregate tested; for instance, the amounts of lithium consumed after 28 days are quite similar for the highly reactive rhyolite and the moderately reactive chloritic schist (reactivity level based on expansion in control concretes), despite the fact that $LiNO_3$ was very effective in controlling concrete expansion with the rhyolite (effective [Li]/[Na + K] = 0.63) and less effective with the schist (effective [Li]/[Na + K] > 0.93; Table 1).

The results from test series no. 4c suggest the formation of a Si–Li reaction product in the form of a finely-dispersed whitish reaction product. In the absence of any XRD analysis and SEM examination, this product could be crystalline or amorphous, expansive or not, and could act as a protective coating. Mechanism C (protective reaction product), mechanism D (crystalline and non expansive reaction product), and mechanism E (non to less expansive amorphous gel), thus remain possible. For its part, mechanism B appears doubtful (unlikely) based on the results obtained in this test series considering that a reaction product is always formed, which most likely contains silicium, in addition to Li.

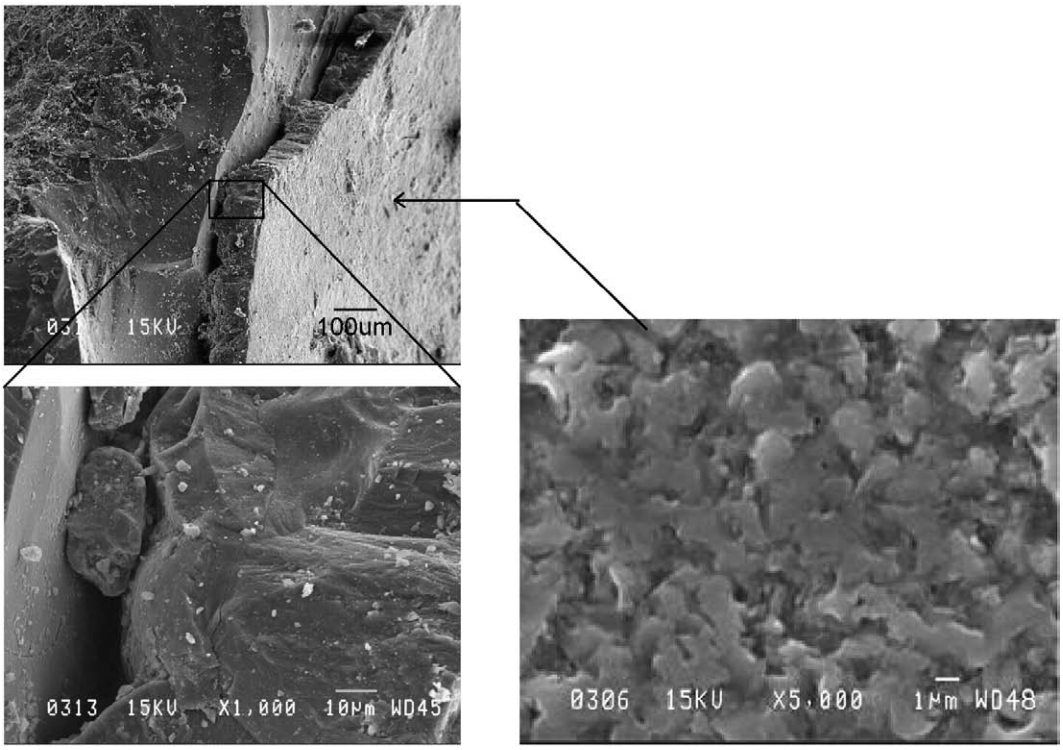

Fig. 4. SEM micrographs at different scales of the Li-silicate layer (Li_2SiO_3) observed on the surface of an obsidian particle immersed for 6 months in a 1 N LiOH solution at 80 °C.

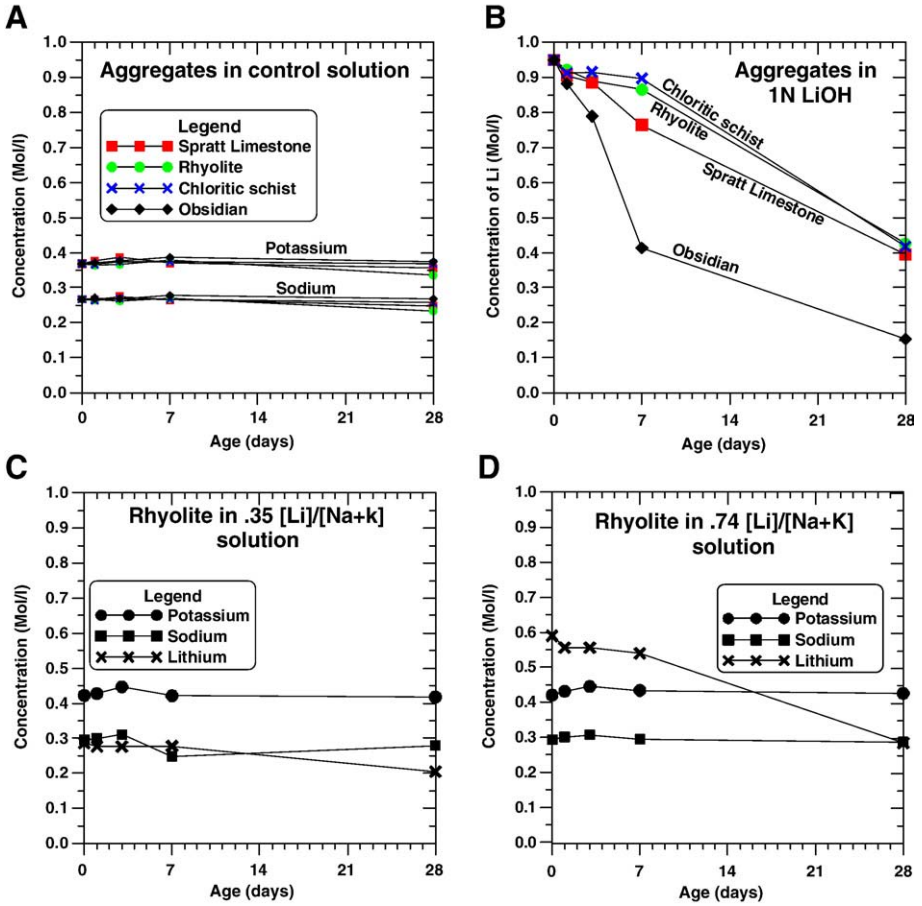

Fig. 5. Alkali concentrations in the soak solution over time when aggregate powders (150–300 µm) were immersed in various Li solutions at 60 °C. (A) All aggregates in 0.68 N (Na,K)OH control solution. (B) All aggregates in 1 N LiOH. (C) Rhyolite in 0.8 N (Na,K)OH + 0.28 N $LiNO_3$ ([Li]/[Na + K] = 0.35). (D) Rhyolite in 0.8 N (Na,K)OH + 0.59 N $LiNO_3$ ([Li]/[Na + K] = 0.74).

3.7. Dissolution of particles of volcanic glass (obsidian), silica varieties, silicate minerals, and natural aggregates immersed for 28 days in various Li-bearing solutions at 80 °C (test series no. 4d)

3.7.1. Immersion in 1 N NaOH control solution

All reactive materials immersed for 28 days in the control solution at 80 °C presented significant mass losses (Table 3). The extremely reactive opal (amorphous silica) and the three highly reactive cryptocrystalline varieties of quartz (chalcedony, red chert, green chert) were completely dissolved after 2, 14, 15, and 15 days, respectively. For all materials tested, dissolution occurred without the formation of any reaction product, thus suggesting that the dissolved silica remained in solution, likely because of the high quantity of solution involved (not saturated with respect to silica) and/or the absence of calcium in the system. Nevertheless, when the percentage of dissolution was important (in the absence of lithium), a translucent colloidal material, likely a silica gel, was generally observed in the test solution.

3.7.2. Immersion in Li-bearing solutions

On the other hand, the presence of lithium in the soak solution reduced the dissolution of all reactive materials tested (except obsidian), often dramatically, in fact for most reactive aggregates tested and the three varieties of cryptocrystalline quartz, i.e. chalcedony, red chert, and green chert (Table 3). In the presence of lithium and reactive material, a finely-dispersed whitish product, amorphous according to XRD and likely containing Li and Si, was always observed at the bottom of the test containers, unless no dissolution (i.e. mass loss) was observed; the higher the dissolution, the more abundant this product.

For chalcedony, a [Li]/[Na] of 0.2 in the soak solution (i.e. 1 N NaOH + 0.2 N $LiNO_3$) decreased the dissolution from 100 wt.% (complete dissolution in the NaOH control solution) to 11 wt.% after 28 days, while a ratio of 0.3 was almost sufficient to largely prevent the dissolution of the particle (Fig. 6A). This value of 0.3 is close to the [Li]/[Na + K] found at equilibrium in the pore solution of a concrete made with a [Li]/[Na + K] mixture ratio of 0.74 [9]. Crystalline Li_2SiO_3 was detected by XRD on the chalcedony surface even when large amounts of lithium were present in the system (Fig. 7). However, it was not possible to observe this Li-silicate when using a 10× magnification lens, likely because the coating was very thin. This assumption is supported by the fact that the underlying chalcedony (cryptocrystalline quartz) is also well-detected by XRD (Fig. 7). Based on these results, i.e. no significant dissolution in the presence of sufficient quantity of $LiNO_3$, and reaction products just in tiny amounts and likely too thin to act as an effective/physical barrier, it is very likely that the presence of lithium in sufficient amounts was very effective in largely suppressing the dissolution of this highly reactive phase. After 28 days in the 1 N NaOH + 0.5 N $LiNO_3$ solution, a particle of chalcedony, mostly unreacted (no significant dissolution in this solution) and just covered with a very thin layer of Li_2SiO_3, was immersed in the 1 N NaOH control solution; the particle then started to dissolve at a rate (~12 wt.% per day, with complete

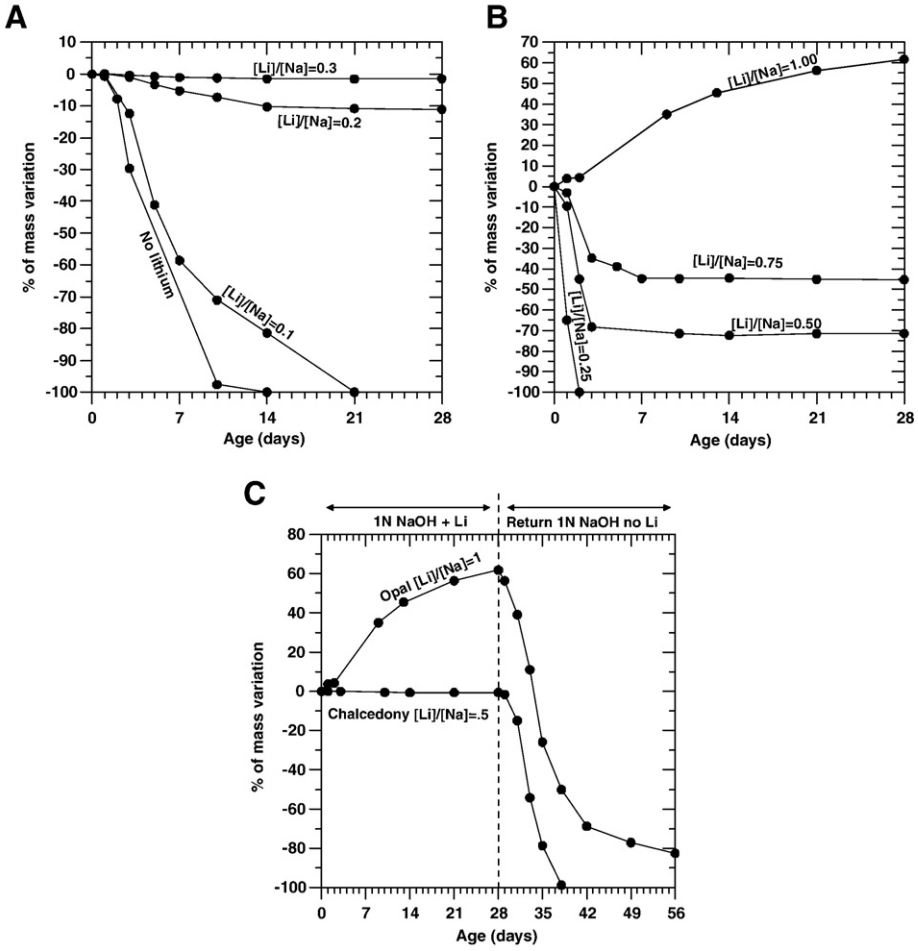

Fig. 6. Mass variation of chalcedony and opal particles immersed at 80 °C in solutions of 1 N NaOH (control) and 1 N NaOH + $LiNO_3$ in various amounts ([Li]/[Na] from 0 to 1.0). (A) Chalcedony. (B) Opal. (C) Chalcedony and opal particles immersed for 28 days in a solution of 1 N NaOH + 0.5 N $LiNO_3$ (chalcedony) or 1.0 N $LiNO_3$ (opal), then immersed in the 1 N NaOH control solution.

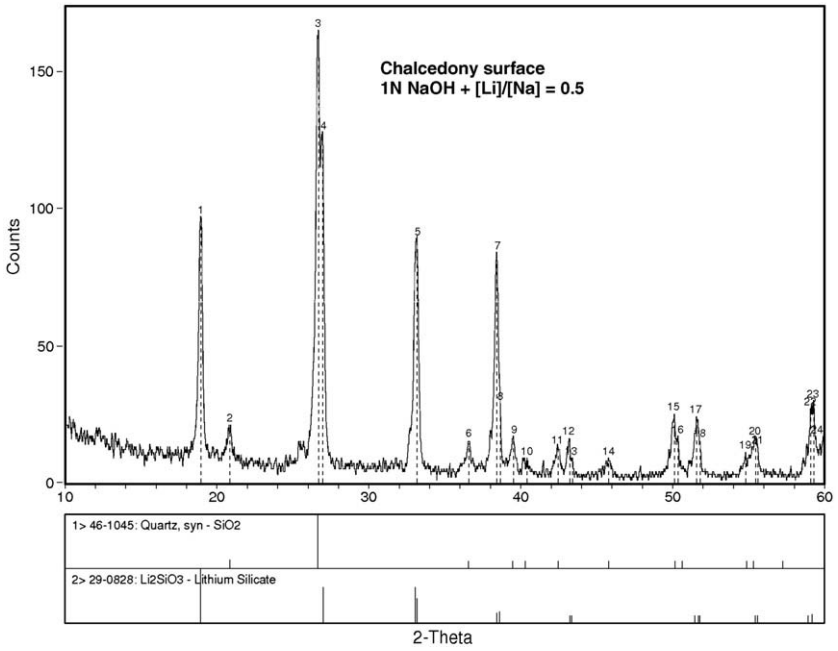

Fig. 7. XRD analysis of the crystalline lithium silicate Li_2SiO_3 (ICDD card file 29-0828) detected on the surface of a chalcedony particle after immersion for 28 days in a 1 N NaOH + 0.5 N $LiNO_3$ solution at 80 °C.

dissolution occuring after 8 days; Fig. 6C) very similar to the dissolution rate of the chalcedony particle initially immersed in the NaOH control solution (~10 wt.% per day for the first 8 days; Fig. 6A). This confirms, once again, that chalcedony does not significantly react or dissolve when the Li concentration is sufficiently high in solution.

It was more difficult to prevent dissolution in the case of opal, by far the most reactive material tested. In the 1 N NaOH + 0.25 N $LiNO_3$ solution ([Li]/[Na + K] = 0.25), the opal particle completely dissolved after 2 days (Fig. 6B) and the finely-dispersed whitish product mentioned above was observed in significant amounts at the bottom of the test containers. In the 1 N NaOH + 0.5 N $LiNO_3$ solution ([Li]/[Na + K] = 0.5), the mass of the particle tested decreased by about 70 wt.% after 3 days, then remained constant afterwards; a finely-dispersed whitish reaction product was also observed, however in relatively smaller amounts. Interestingly, a naked-eye visible compact layer of secondary reaction product, also observed by Yin and Wen [18], formed around the reacting particle. This product was found to be amorphous based on XRD. In actual fact, the opal grain completely dissolved after about 3 days, then leaving a particle essentially made of an empty shell of amorphous reaction product weighing about 30% of the original mass (overall mass loss of 70 wt.%; Fig. 6B). The same observations were made for the particle immersed in the 1 N NaOH + 0.75 N $LiNO_3$ solution ([Li]/[Na + K] = 0.75) except that: (1), the opal completely dissolved after about 7 days, (2), leaving a residual empty shell of reaction product corresponding to about 55 wt.% of the initial mass (overall mass loss of 45 wt.%; Fig. 6B), and (3), the amount of finely-dispersed whitish product was again smaller. In the 1 N NaOH + 1 N $LiNO_3$ solution ([Li]/[Na + K] = 1.0), a mass gain of over 60 wt.% was rather observed. In this particular case, the finely-dispersed whitish product was absent; the opal again dissolved completely but the totality of the dissolved silica precipitated as the reaction shell. The 60 wt.% increase in mass is explained by the fact that this shell is composed of a hydrous and hydrated amorphous material which, in addition to the totality of the silica from the reacted opal, incorporated other substances from the solution (e.g. lithium, OH radicals, water molecules, and possibly also some NO_3). The two amorphous products formed (residual shell and finely-dispersed whitish product) have not been chemically analysed, but they could correspond to the same reaction product. It is thus obvious that the layer of reaction product around the original opal particle did not protect the underlying opal against dissolution; nevertheless, Fig. 6B suggests that the more important the thickness of this layer (which progressively increases from 0.5 to 1.0 N $LiNO_3$), the slower the rate of dissolution. After 28 days in the 1 N NaOH + 1.0 N $LiNO_3$ solution ([Li]/[Na + K] = 1.0), the residual opal particle, in fact totally composed of an amorphous reaction product, was immersed in the 1 N NaOH control solution (Fig. 6C). The particle progressively dissolved, however at a much lower rate (<10 wt.% per day) than the opal particle initially immersed in the control solution (100 wt.% dissolution after two days). This demonstrates that the reaction product also remains highly susceptible to dissolve in the 1 N NaOH solution (in the absence of lithium), however less than the original opal. The opal thus behaved differently in many respects from chalcedony and most other reactive materials tested (except obsidian). The presence of lithium did reduce its dissolution, but the silica dissolved was largely and more or less rapidly incorporated into amorphous Si–Li reaction products (surrounding shell and whitish product finely-dispersed in the soak solution), depending upon the lithium concentration. The higher this concentration, the lower the mobility of the silica dissolved, the higher the amount of reaction product formed close to the reaction site (e.g. in the shell), and the lower the amount of finely-dispersed whitish product in the test solution.

Obsidian, a totally amorphous volcanic glass, also performed differently from most other reactive materials tested. As for opal, lithium does not seem to reduce dissolution (Table 3), which, however, never exceeded 10 wt.% (mass loss), and no crystalline product was detected on its surface by XRD; the finely-dispersed whitish product mentioned above and observed at the bottom of the test containers was found to be the only product formed in the presence of lithium.

The same whitish secondary product was also observed with the three feldspars tested (microcline, orthoclase, and anorthite) after immersion in the LiOH solution without, however, any significant dissolution reduction with respect to the control solution (Table 3). Evenmore, obsidian, anorthite, and microcline suffered more dissolution in the 1 N LiOH solution than in the 1 N NaOH control solution (Table 3), which cannot be explained for the time being.

3.7.3. Discussion

Globally, the results from the test series no. 4d support mechanism B relating to reduction/suppression of silica dissolution due to another mechanism than pH reduction (i.e. mechanism A) or, to some extent, the early formation of a protective reaction product on the reactive silica grains or aggregate particles (i.e. mechanism C). Indeed, most reactive materials presented dramatic dissolution reductions in the presence of Li, except the extremely reactive opal (lower reductions) and the highly reactive volcanic glass (obsidian), for which the dissolution was almost unchanged in the NaOH + $LiNO_3$ solution (−7.0 wt.% vs. −7.8 wt.% in the control solution; Table 3) and even increased in the LiOH solution (−10.2 wt.%; Table 3). For its part, mechanism E remains possible: when silica dissolution was not completely stopped in the presence of lithium, amorphous Si–Li reaction products in the form of a finely-dispersed whitish product was observed, in amounts proportional to dissolution (except for opal where two amorphous products were found i.e. the finely-dispersed material and the surrounding shell); however, the non to less expansive character of this amorphous reaction product is unknown. On the other hand, mechanisms C and D are unlikely. In the first case, when a significant coating of reaction product was observed on the reactive particles, in fact just for opal, this coating was not protecting the underlying reactive phase from further dissolution. In the second case, a well-crystallized Li silicate was only observed at the surface of chalcedony, with no significant dissolution, but this deposit was very thin.

It is not easy to draw conclusive statements about the effect of the lithium on the different types of reactive aggregate/material tested. For instance: (1), two of the highest dissolution (mass loss) values after 28 days in the control solution correspond to aggregates with one of the highest (rhyolite: 7.8 wt.%; Table 3) and the lowest (granitic rock: 7.8 wt.%; Table 3) expansions in (control) concrete [9]; (2), concrete expansion due to ASR in the presence of the above two aggregates is easily controlled with $LiNO_3$ (effective [Li]/[Na + K] < 0.74; [9]); nevertheless, these two aggregates also present the two highest dissolution values after 28 days in the 1 N NaOH + 0.25 N $LiNO_3$ solution (1.3 wt.% for both; Table 3); (3), the lowest dissolution value (0.1 wt.%) in the same solution corresponds to an aggregate (chloritic schist) for which $LiNO_3$ is not highly effective in concrete (effective [Li]/[Na + K] > 0.93; [9]) and so on. However, it may be of interest for further research to note that: (1), all 5 reactive silicate aggregates tested (rhyolite, greywacke, granitic rock, chloritic schist, and quartzitic sandstone) dissolved less or not more in the 1 N NaOH + 0.25 N $LiNO_3$ solution than in the 1 N LiOH solution, despite a lower Li content, and (2), at the opposite, the two calcite-rich reactive limestones tested dissolved less in the 1 N LiOH solution than in the two NaOH + $LiNO_3$ solutions tested.

According to Feng et al. [28], the differences in the $LiNO_3$ effectiveness observed for concretes incorporating the rhyolite (effective [Li]/[Na + K] = 0.63 according to Tremblay et al. [9], and 0.74 according to Feng et al. [28]) and the greywacke (effective [Li]/[Na + K] > 1.11 according to Tremblay et al. [9], and 1.48 according to Feng et al. [28]), could be attributed to textural differences between the two types of aggregates; this would cause the reactive silica to be more rapidly accessible from the rhyolite (which contains 85 vol.% devitrified glass) than from the greywacke (which contains about 8 vol.% microcrystalline quartz). However, in the present study, the two aggregates showed very similar dissolution values in all test solutions, including the NaOH control solution (see Table 3 for 28-day results).

3.8. General discussion

The most realistic and conclusive experiments carried out in this study and summarized in Table 4 are those performed on concrete specimens stored in air at high humidity and relatively low temperatures (38 °C and 60 °C), and incorporating natural reactive aggregates (i.e. test series nos. 1 and 2), followed by the experiments on composite specimens made of reactive aggregate particles and cement paste immersed in a NaOH + $LiNO_3$ solution at 80 °C (test series no. 3). Conclusions based on these tests, which strongly support or disprove one or more of the mechanisms proposed, call for greater consideration. For their part, the immersion test series nos. 4a to 4d were all performed in the absence of cement and at relatively high temperatures (60, 80, or 350 °C). The corresponding results must thus be used with circumspection, particularly those obtained at 350 °C (autoclave), in LiOH solution, and/or for extremely to highly reactive materials such as opal, fused silica, chalcedony, chert, and obsidian. Such materials are uncommon in real concretes, at least in significant amounts, while they often performed very differently in some test series with respect to the natural reactive aggregates tested in parallel.

Up to now, for each test series taken individually, each mechanism proposed has been considered “likely”, “possible”, “non-conclusive”, “unlikely”, or “impossible”, based on the results obtained and the rationale summarized in Table 4. It remains to draw the global conclusion described hereafter regarding each of the mechanisms considered.

Mechanism B, i.e. chemical stability of reactive silica increased for another reason than pH reduction (i.e. mechanism A) or early formation of a protective coating on the reactive silica grains or aggregate particles (i.e. mechanism C), is the mechanism among all those considered in this study that better explains the effectiveness of $LiNO_3$ against ASR. This mechanism is supported (i.e. considered “likely”) by test series nos. 2, 3, and 4d, however disproved (i.e. considered “unlikely”) by the test series no. 4c (Table 4). This mechanism is strongly supported by the fact that all reactive materials tested in test series 4d (including 7 reactive aggregates) dissolved much less in LiOH and NaOH + $LiNO_3$ solutions than in a NaOH control solution, with only one exception (obsidian). Mechanism A, i.e. chemical stability of reactive silica increased due to pH reduction, and mechanism F, i.e. expansion reduced/suppressed due to higher solubility of silica but that remains in solution, are considered impossible, based on pore solution chemistry (test series no. 1). Mechanism C, i.e. chemical stability of reactive silica increased due to the early formation of a protective coating over the reactive silica grains or aggregate particles, disproved by 3 test series while not supported by any other, is unlikely. Mechanism D, i.e. expansion reduced/suppressed due to formation of a non expansive Si–Li crystalline reaction product, disproved by 4 test series while not supported by any other, is also unlikely. Mechanism E, i.e. expansion reduced/suppressed due to the formation of a non or less expansive Si–Li amorphous gel, disproved by two test series while not supported by any other, remains possible, at the most. The three mechanisms C, D, and E, are particularly disproved following the examination of the concrete specimens (test series no. 2), which rather suggests that the only reaction product formed, and this only when lithium is not highly effective, contains lithium, looks like classical ASR gel, and is expansive as well.

It was already well established that the effectiveness of $LiNO_3$ against ASR varies from one reactive aggregate to another, irrespective of their inherent degree of reactivity (i.e. expansivity in concrete prism tests) [9]. An important subject of concern in this study is how the nature of the particular reactive aggregate to counteract can affect the effectiveness of $LiNO_3$ in increasing the chemical stability of reactive silica. Unfortunately, none of the experiments performed in this study led to conclusive results in this respect. At the very least, the dissolution tests (series 4d) proved that the capacity of lithium in reducing the rate of silica dissolution greatly varies with the type of reactive silica involved.

In numerous studies relating to ASR, extremely to highly reactive natural or synthetic materials, which are rarely used as concrete aggregates, are often tested, such as opal, chalcedony, chert, volcanic

glass (e.g. obsidian), fused silica, pyrex, and so on. As clearly demonstrated in the present study, such rather unusual materials may behave very differently from natural reactive aggregates (e.g. opal and obsidian in this study), particularly when they are tested as very fine particles. This thus recalls the importance of testing real reactive aggregates under usual particle size distributions, to be more realistic.

4. Conclusions

Numerous sets of experiments were carried out with the objective of determining which mechanisms(s) better explain the effectiveness of $LiNO_3$ against ASR, and variations in this effectiveness as well with the type of reactive aggregate to counteract. These experiments included: (1), pore solution chemistry of cement pastes and concretes incorporating $LiNO_3$ and various reactive and non reactive aggregates; (2), visual examination and microanalysis of the above concretes; (3), immersion of composite specimens made of reactive aggregates and cement paste in a $NaOH + LiNO_3$ solution, and (4), immersion of particles of various reactive aggregates, silica phases, silicates, and volcanic glass, in various Li-bearing solutions (LiOH, $NaOH + LiNO_3$) at various temperatures (60 °C, 80 °C, and 350 °C in the autoclave).

Six different mechanisms proposed to explain the beneficial effect of $LiNO_3$ against ASR were considered and critically examined against the results of the above experiments, which can be grouped in two main categories:

(1) chemical stability of reactive silica increased (i.e. compared to solution without lithium) due to: pH decrease in the concrete pore solution (mechanism A), other change(s) in the chemistry of the pore solution (mechanism B), or early formation, over the reactive silica grains or aggregate particles, of a Si–Li reaction product which acts as a physical barrier against further reaction (mechanism C);
(2) chemical stability of silica almost unchanged or remaining significant, but concrete expansion significantly reduced or suppressed due to: formation of a crystalline and non expansive Si–Li reaction product (mechanism D), formation of an amorphous Si–Li reaction product (i.e. a gel) that is non expansive or less expansive than the classical ASR gel (mechanism E), or increased solubility of silica, which thus mostly remains in solution without forming an expansive gel (mechanism F).

The following conclusions can be drawn from the results obtained in our studies:

- Mechanisms A (pH reduction) and F (increased solubility of silica) are not supported based on the pore solution chemistry results which showed that the pH was not significantly reduced in the concrete pore solution in the presence of $LiNO_3$ and that the silica concentration in solution was always low and not affected by the presence of $LiNO_3$.
- Mechanism C (protective coating) is considered unlikely. In the presence of $LiNO_3$, reaction products were not observed at the surface of or somehow surrounding the reactive phases in all investigated concretes and composite specimens made of cement paste and reactive particles. A layer of well-crystallized Li_2SiO_3 has been observed on the surface of obsidian and a number of reactive aggregate particles but following immersion in a LiOH solution at 350 °C in the autoclave (also at 80 °C for obsidian). However, in the presence of $LiNO_3$, a (very thin) layer of such a lithium-bearing silicate has been only observed at the surface of chalcedony particles immersed in $NaOH + LiNO_3$ solutions at 80 °C, the protective character of this layer being doubtful, while a clearly non-protective layer of an amorphous reaction product has been only observed at the surface of opal particles immersed in the same solutions.
- Mechanism D (non expansive crystalline product) is also considered unlikely. In the presence of $LiNO_3$, crystalline reaction products were not observed in any of the investigated concretes and composite specimens made of cement paste and reactive particles. In fact, in the presence of $LiNO_3$, as just mentioned, a likely non expansive crystalline reaction product (i.e. Li_2SiO_3) was only detected in tiny amounts at the surface of unreacted chalcedony particles immersed in $NaOH + LiNO_3$ solutions at 80 °C.
- Mechanism E (non to less expansive amorphous gel) is also unlikely. This mechanism is strongly disproved by the direct examination of concrete specimens which rather suggest that the only reaction product formed, when $LiNO_3$ is present in insufficient amounts/dosage, contains lithium, looks like classical ASR gel, and is expansive as well. In fact, an amorphous reaction product in the form of a finely-dispersed whitish product was observed in some immersion tests but its non to less expansive character is unknown.
- Mechanism B (increased chemical stability of reactive silica due to another reason than pH reduction or early formation of a protective coating) is the mechanism among all those investigated in this study that seems to better explain the effectiveness of $LiNO_3$ against ASR, and the variations in this effectiveness (i.e. extent of expansion reduction) from one reactive aggregate to another. This mechanism is strongly supported by the facts that: (1), an amorphous gel containing Na, K, and Si, and likely also Li (undetectable under the SEM), was the only type of reaction product observed in concrete specimens incorporating $LiNO_3$ and a variety of natural reactive aggregates; (2), this gel was looking exactly like the classical ASR gel and its abundance was somewhat proportional to the concrete expansion attained; for instance, for all concretes made with $LiNO_3$ and showing no or limited expansion, no or only traces of reaction gel were observed; and (3), most reactive materials tested, including all the 8 natural reactive aggregates tested, dissolved much less in $NaOH + LiNO_3$ (and LiOH) solutions than in a NaOH control solution.
- Some of the most reactive materials tested in this study, (e.g. opal and obsidian), which are quite unusual in concrete aggregates, may behave very differently from natural reactive aggregates, particularly when they are tested as very fine particles. This arises the importance of testing natural reactive aggregates under realistic particle size distributions.
- It is still unknown how the presence of $LiNO_3$ in the concrete pore solution can increase the stability of reactive silica and how this phenomenon can be affected by the particular reactive aggregate to counteract, irrespective of its petrographic nature and inherent reactivity (based on expansivity in control concretes).

Acknowledgements

Euclid Admixtures Canada Inc., the Fonds Québécois de la Recherche sur la Nature et les Technologies of Québec (FQRNT), and the Natural Science and Engineering Research Council of Canada (NSERC), are greatly acknowledged for their financial support.

References

[1] S. Diamond, ASR — another look at mechanisms, in: K. Okada, S. Nishibayashi, M. Kawamura (Eds.), Proceedings of the 8th International Conference on AAR, Society of Materials Sciences, Kyoto, 1989, pp. 83–94.
[2] P. Longuet, L. Burglen, A. Zelmer, La phase liquide du ciment hydrate, Rev. Matér. 676 (1973) 35–41.
[3] T. Ichikawa, M. Miura, Modified model of alkali-silica reaction, Cem. Concr. Res. 37 (2007) 1291–1297.
[4] L.S. Dent-Glasser, N. Kataoka, The chemistry of alkali-aggregate reaction, Proceedings of the 5th International Conference on AAR, National Building Research Institute, Cape-Town, South-Africa, 1981, paper S252 (23 pp.).
[5] M.A. Bérubé, B. Fournier, Les produits de la reaction alkalis-silice dans le béton - Étude de cas de la région de Québec, Can. Mineral. 24 (1986) 271–288.
[6] W.J. McCoy, A.G. Caldwell, New approach in inhibiting alkali-aggregate expansion, ACI Mater. J. 22 (9) (1951) 693–706.
[7] X. Feng, M.D.A. Thomas, T.W. Bremner, B.J. Balcom, K.J. Folliard, Studies on lithium salts to mitigate ASR-induced expansion in new concrete: a critical review, Cem. Concr. Res. 35 (9) (2005) 1789–1796.

[8] C. Tremblay, M.A. Bérubé, B. Fournier, M.D.A. Thomas, D.B. Stokes, Performance of lithium-based products against ASR: application to Canadian aggregates, reaction mechanisms, and testing, in: M. Tang, M. Deng (Eds.), Proceedings of the 12th International Conference on AAR, International Academic Publishers, Beijing, 2004, pp. 668–677.
[9] C. Tremblay, M.A. Bérubé, B. Fournier, M.D.A. Thomas, K.J. Folliard, Effectiveness of lithium-based products in concrete made with Canadian aggregates susceptible to ASR, ACI Mater. J. 104 (2) (2007) 195–205.
[10] D.B. Stokes, H.H. Wang, S. Diamond, A lithium-based admixture for ASR control that does not increase the pore solution pH, in: V.M. Malhotra (Ed.), Proceedings of the 5th CANMET/ACI International Conference on Superplastisizers and Other Chemical Admixtures in Concrete, American Concrete Institute, ACI SP 173, 1997, pp. 855–868.
[11] S. Diamond, Unique response of $LiNO_3$ as an alkali silica reaction-preventive admixture, Cem. Concr. Res. 29 (8) (1999) 1271–1275.
[12] M.A. Bérubé, C. Tremblay, B. Fournier, M.D. Thomas, D.B. Stokes, Influence of lithium products proposed for counteracting ASR on the chemistry of cement hydrates and pore solution, Cem. Concr. Res. 34 (2004) 1645–1660.
[13] M. Lawrence, H.F. Vivian, The reactions of various alkalies with silica, Aust. J. Appl. Sci. 12 (1961) 96.
[14] P.W.J.G. Wijnen, T.P.M. Beelen, J.W. De Haan, C.P.J. Rummens, L.J.M. Van De Ven, R.A. Van Santen, Silica gel dissolution in aqueous alkali metal hydroxides studies by 29Si NMR, J. Non-Cryst. Solids 109 (1989) 85–94.
[15] C.L. Collins, J.H. Ideker, G.S. Willis, K.E. Kurtis, Examination of the effects of LiOH, LiCL, and $LiNO_3$ on alkali-silica reaction, Cem. Concr. Res. 34 (2004) 1403–1415.
[16] X. Feng, M.D.A. Thomas, T.W. Bremner, B.J. Balcom, K.J. Folliard, Effect of $LiNO_3$ on ASR-expansion and dissolution of silica, in: B. Fournier (Ed.), Marc-André Bérubé Symposium on Alkali-Aggregate Reactivity in Concrete, Montréal, Canada, 2006, pp. 139–152.
[17] L.D. Mitchell, J.J. Beaudoin, P. Grattan-Bellew, The effects of lithium hydroxyde solution on alkali silica reaction gels created with opal, Cem. Concr. Res. 34 (4) (2004) 641–649.
[18] Q. Yin, Z. Wen, Effects of lithium hydroxide on alkali silica reaction gels, in: M. Tang, M. Deng (Eds.), Proceedings of the 12th International Conference on AAR, International Academic Publishers, Beijing, China, 2004, pp. 801–804.
[19] Y. Sakaguchi, M. Takakura, A. Kitagawa, T. Hori, F. Tomosawa, M. Abe, The inhibiting effect of lithium compounds on ASR, in: K. Okada, S. Nishibayashi, M. Kawamura (Eds.), Proceedings of the 8th International Conference on AAR, Society of Materials Sciences, Kyoto, 1989, pp. 229–234.
[20] S. Diamond, S. Ong, The mechanisms of lithium effects on ASR, Proceedings of the 9th International Conference on AAR, London, UK, 1992, pp. 269–278.
[21] X. Mo, C. Yu, Z. Xu, Long-term effectiveness and mechanism of LiOH in inhibiting alkali silica reaction, Cem. Concr. Res. 33 (1) (2003) 115–119.
[22] K.E. Kurtis, P.J.M. Monteiro, Chemical additives to control expansion of alkali-silica reaction gel: proposed mechanisms of control, J. Mater. Sci. 38 (2003) 2027–2036.
[23] M. Prezzi, P.J.M. Monteiro, G. Sposito, Alkali-silica reaction — Part 1: use of the double-layer theory to explain the behavior of the reaction product gels, ACI Mater. J. 94 (1) (1997) 10–17.
[24] M. Prezzi, P.J.M. Monteiro, G. Sposito, Alkali-silica reaction — Part 2: the effect of chemical admixtures, ACI Mater. J. 95 (1) (1998) 3–10.
[25] Canadian Standards Association (CSA), Potential expansivity of aggregates, procedure for length change due to alkali-aggregate reaction in concrete prisms, CAN/CSA standard A23.2–14A, CSA International, Mississauga, ON, Canada, 2004.
[26] American Society for Testing and Materials (ASTM), Standard test method for determination of length change of concrete due to alkali-silica reaction, ASTM Standard C1293, ASTM International, West Conshohocken, PA, USA, 2006.
[27] American Association of State and Highway Transportation Officials (AASHTO), Standard method of test for rapid identification of alkali-silica reaction products in concrete, AASHTO standard T 299, 1993 Washington, DC, USA.
[28] X. Feng, M.D.A. Thomas, T.W. Bremner, B.J. Balcom, K.J. Folliard, B. Fournier, Summary of research on the effect of $LiNO_3$ on alkali-silica reaction in new concrete, Proceedings of the 13th International Conference on AAR, Trondheim, Norway, 2008, 9 pp.